Pergamon

0967–0637(95)00012–7

Deep-Sea Research I, Vol. 42, No. 4, pp. 477–500, 1995

0967–0637/95 $9.50 + 0.00

Effect of Drake Passage on the global thermohaline circulation

J. R. TOGGWEILER* and B. SAMUELS*

(*Received* 4 *November* 1993; *in revised form* 30 *June* 1994; *accepted* 6 *July* 1994)

Abstract—The Ekman divergence around Antarctica raises a large amount of deep water to the ocean's surface. The regional Ekman transport moves the upwelled deep water northward out of the circumpolar zone. The divergence and northward surface drift combine, in effect, to remove deep water from the interior of the ocean. This wind-driven removal process is facilitated by a unique dynamic constraint operating in the latitude band containing Drake Passage. Through a simple model sensitivity experiment we show that the upwelling and removal of deep water in the circumpolar belt may be quantitatively related to the formation of new deep water in the northern North Atlantic. These results show that stronger winds in the south can induce more deep water formation in the north and more deep outflow through the South Atlantic. The fact that winds in the southern hemisphere might influence the formation of deep water in the North Atlantic brings into question long-standing notions about the forces that drive the ocean's thermohaline circulation.

INTRODUCTION

DRAKE passage is the name given to the opening between the southern tip of South America (56°S) and the northern tip of Palmer Peninsula in West Antarctica (62°S). Drake Passage connects the Atlantic and Pacific Oceans and provides for the only continuous zonal band of water in the modern ocean (apart from the Arctic Ocean north of 84°N). In a latitude band with no continental barriers, east–west pressure gradients averaged around the globe must be zero. This offers a strong constraint to the meridional flow, i.e. there can be no net geostrophically balanced north–south flow in such a band.

In one of the earliest scientific papers written about the results of an ocean general circulation model, GILL and BRYAN (1971) described the effect of Drake Passage on the thermally driven overturning in the southern hemisphere. With Drake Passage blocked up, the upper (poleward) branch of the overturning extends southward to Antarctica, where the upper ocean flow is cooled and sinks. It then flows back into the interior as a near-bottom current and finally upwells back toward the surface in low latitudes. With Drake Passage open, the thermally driven upper ocean flow cannot cross or pass into the latitude band of Drake Passage. The main region of sinking and bottom water formation shifts to the latitudes north of Drake Passage. Similar results were illustrated by Cox (1989).

Winds blowing over the latitude band of Drake Passage produce another important effect. The circumpolar westerlies drive a northward Ekman drift in the near surface layers. Because the Ekman drift is not geostrophically balanced, it is not affected by the

*Geophysical Fluid Dynamics Laboratory/NOAA, P.O. Box 308, Princeton, NJ 08542, U.S.A.

existence of Drake Passage. But any subsurface return flow balancing the surface drift should be subject to the constraint on geostrophic flow. A net poleward geostrophic flow balancing the Ekman drift can only exist at depths where there are topographic ridges to support east–west pressure gradients. The topographic features relevant to this problem are Scotia Arc in the South Atlantic, Kerguelen Plateau in the Indian Ocean, and the Macquarie Ridge, south of New Zealand. These features can support poleward return flows only at depths below ~1500 m.

The idea of a coupling between the surface Ekman layer and a deep poleward flow has appeared in the literature on several occasions. In discussing the momentum budget for the Antarctic Circumpolar Current (ACC), MUNK and PALMEN (1951) speculated that a deep poleward flow balancing the surface Ekman drift might act to transfer momentum from the surface Ekman layer into the bottom topography. DESZOEKE and LEVINE (1981) showed that the meridional heat flux associated with the Ekman drift and its compensating deep flow is small and equatorward. A northward flow of 2–3°C surface water overlying a poleward flow of ~1.5°C deep water produces a small net equatorward heat flux. This small equatorward heat flux is a far cry from the large advective heat flux that would exist if Drake Passage were closed and warm upper ocean water could flow directly down to Antarctica.

WARREN (1990) analysed the water mass and density structures which are found in proximity to the topographic ridges in the latitude band of Drake Passage. He then used the Drake Passage constraint on geostrophic flow to explain why convective processes around Antarctica are apparently unable to ventilate oxygen-poor deep layers north of Drake Passage. Warren also points out that the water mass which sits just below the tops of the topographic ridges, as if poised to flow poleward in geostrophic balance, is none other than North Atlantic Deep Water (NADW).

In this paper, we point out another far-reaching effect of the coupling between the Ekman layer and its deep poleward return flow. The surface winds in the circumpolar belt are strongest near 50°S, i.e. just north of Drake Passage. The zonal wind stress tapers off to the south such that the Ekman transport in the latitude band of Drake Passage is divergent, drawing ~15 Sv into the surface Ekman layer south of the tip of South America (HELLERMAN and ROSENSTEIN, 1983). Because the divergence south of the tip of South America cannot be fed by shallow water, it draws deep water up from the level of the topographic ridges. This is important because the surface water flowing northward out of the latitude band of Drake Passage and the deep water flowing poleward to replace it are widely separated in density. Thus, the winds, in drawing deep water up to the surface, force a conversion of dense, deep water into light (mainly fresher) surface water. The winds, in effect, remove ~15 Sv of deep water from the interior of the ocean.

In the light of the above, WARREN's (1990) connection between North Atlantic Deep Water and the Drake Passage constraint seems especially pertinent. A process somewhere else in the ocean must balance the conversion of 15 Sv of deep water into 15 Sv of surface water in the circumpolar belt. It is well known that ~20 Sv of upper ocean water is converted to deep water in the North Atlantic (BROECKER, 1991). Indeed, the North Atlantic is the only place north of the tip of South America where upper ocean water is converted to deep water in these quantities.

Oceanographers usually think of the formation of North Atlantic Deep Water as the quintessential example of an overturning circulation driven by thermohaline processes. This paper entertains the idea that the magnitude of NADW outflow from the Atlantic

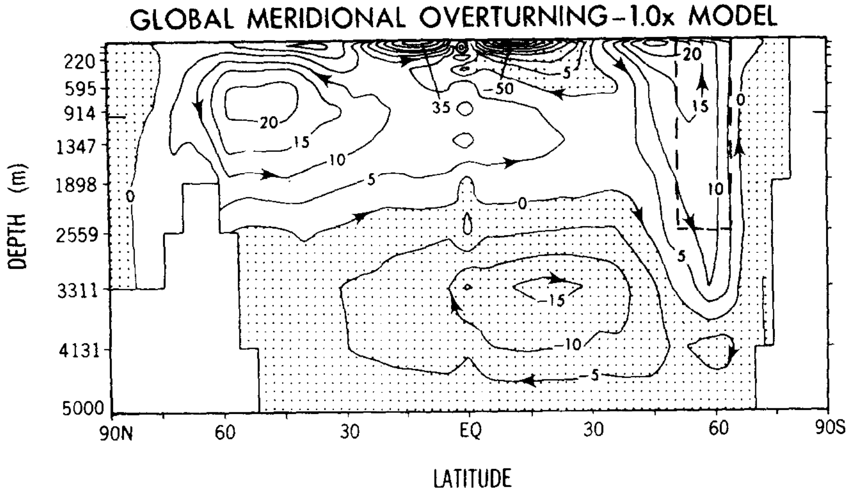

Fig. 1. Global meridional overturning transport stream function from the standard 1.0× model. The flow between stream lines is 5×10^6 m^3 s^{-1}. The dashed box centered on 60°S shows the depth and latitudinal extent of the model's topographic gap between South America and Antarctica.

basin may be dictated by the wind stress in the latitude band of Drake Passage. The feasibility of such a linkage will be demonstrated using a low-resolution ocean general circulation model. Please consider the phrase "Drake Passage effect" as a specific reference to this linkage.

MODEL RESULTS

The ocean circulation model used in these experiments is based on the GFDL Modular Ocean Model ("MOM") version 1.0 (PACANOWSKI *et al.*, 1991). The configuration and parameter set used by this particular model is derived from earlier studies by BRYAN and LEWIS (1979) and TOGGWEILER *et al.* (1989a). The model has a coarse resolution (4.5° latitude × 3.75° longitude × 12 vertical levels) and is forced by annual mean boundary conditions at the surface. The wind stress field is based on HELLERMAN and ROSENSTEIN (1983). Predicted temperatures and salinities in the model's upper most layer ($\Delta z = 51$ m) are restored toward the temperature and salinity data in LEVITUS (1982) averaged over the upper 50 m with time constants of 1/30 day^{-1} for temperature and 1/120 day^{-1} for salinity.

The model's global meridional overturning after 2000 years of integration is illustrated in Fig. 1. The model generates a fairly vigorous meridional circulation with 21 Sv of deep water formation in the North Atlantic and nearly 8 Sv of bottom water flow away from Antarctica. In a model of this resolution, topographic features such as Scotia Arc and the higher elevations of Kerguelen Plateau are not resolved. This leaves the sill between South America and Antarctica as the highest topography encountered in the latitude band of Drake Passage. Figure 1 includes an overlay of the opening between South America and Antarctica. The sill between South America and Antarctica is 2559 m. This is the effective upper limit for a net geostrophically balanced poleward flow.

Figure 2 shows the zonal component of the Hellerman and Rosenstein annual-mean wind stress field. In the southern hemisphere, the zonal wind changes sign from easterly to

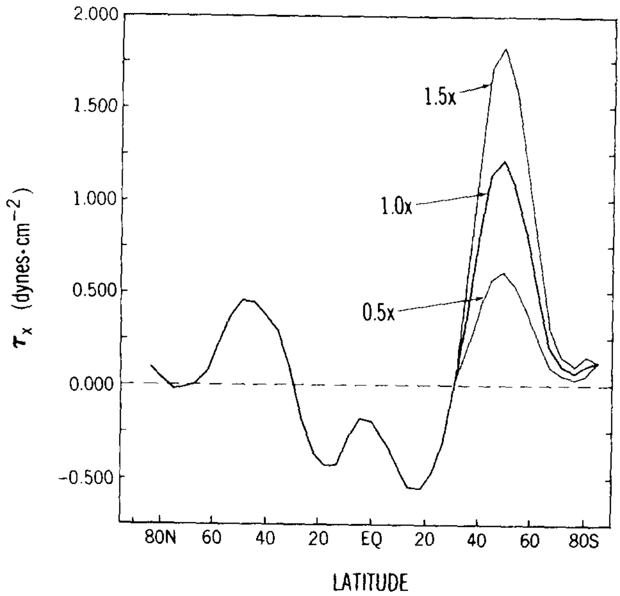

Fig. 2. Mean zonal component of the annual mean wind stress (dynes cm^{-2}) plotted as a function of latitude, after HELLERMAN and ROSENSTEIN (1983). The zonal component of the stress south of 30°S has been multiplied by factors of 0.5, 1.0 and 1.5 to create the wind-sensitivity experiments described in the text.

westerly at 30°S. The model sensitivity test in this paper consists of a simple modification of the zonal wind stress in the westerly band. The zonal stress south of 30°S was multiplied by factors of 0.5, 1.0 and 1.5 and the model was run out with each stress field for ~2000 years. Modifying the stress field in this way alters both the stress magnitude and its latitudinal shear. The restoring of surface temperatures and salinities to observed values remains the same in all three cases. Table 1 summarizes the model experiments described in this paper.

The tip of South America in this low-resolution model is at 51.1°S. In the model with standard winds, 1.0×, the zonally integrated Ekman transport in the first model grid row south of the tip of South America is 22 Sv directed northward. The divergence of the wind stress field south of 51°S raises an equal volume of subsurface water into the surface layer. In Fig. 1 it is apparent that most of the upwelled water comes from depths below 1000 m. At least 10 Sv of the 22 Sv comes from depths below the sill in Drake Passage. We will refer to the zonally integrated Ekman drift at the tip of South America with the notation $\int (\tau_x/f)dx_{SA}$. The quantity $\int (\tau_x/f)dx_{SA}$ is reduced to 11 Sv in the 0.5× case and is increased to 33 Sv in the 1.5× case.

Figure 3 shows the change in meridional overturning in the Atlantic basin produced by changing the wind stress in the south, the main result of this paper. As suggested in the introduction, the overturning circulation in the Atlantic becomes significantly stronger when the wind stress is increased. Basically, stronger winds in the south remove deep water from the interior of the ocean. The North Atlantic is the only place north of Drake Passage where new deep water is formed. A stronger wind forcing in the south causes more upper ocean water to encounter the cold surface boundary conditions in the North Atlantic. More heat is removed from the ocean and more deep water is formed.

Table 1. List of model experiments

Modified wind stress (Standard model)

Zonal wind stress multiplied by 0.5×, 1.0× and 1.5× at every grid point south of 30°S. Each version run out to steady state. Standard model described in text and in TOGGWEILER *et al.* (1989a,b) and TOGGWEILER and SAMUELS (1993a,b).

North Atlantic restore

Interior T and S at all grid points north of 46.7°N in North Atlantic restored toward LEVITUS (1982) annual-mean observations. Restoring time constant = 1/10 y^{-1} (Levels 2–12). Applied to 0.5×, 1.0× and 1.5× versions of standard model. Each case run out to steady state.

Modified North Atlantic T^*

Annual-mean temperatures being restored to (T^*) in model's upper layer reduced by 2.5°C at all grid points north of 46.7°N in the North Atlantic. Applied to 0.5×, 1.0× and 1.5× versions of standard model. Each case run out to steady state.

Idealized tracers

1. Tracer introduced into mid-depths (483–2228 m) of 1.0× version of standard model in zonal strip just north of Drake Passage (37.8°S–51.1°S). Evolution of tracer followed for 200 years.
2. Tracer introduced into surface layer of 1.0× version of standard model in zonal strip within latitude band of Drake Passage (51.1°S–64.5°S). Evolution of tracer followed for 200 years.

Non-sinking North Atlantic (Appendix)

An average of 2 salinity units was subtracted from salinities being restored to (S^*) at all grid points north of 35°N in the North Atlantic in a steady-state run of the standard model.

Figure 3 shows that it is only the overturning which traverses the whole Atlantic basin that is affected by the change in the wind. Each example in Fig. 3 shows that there is an additional ~10 Sv of overturning which recirculates within the North Atlantic. The recirculating component does not change when the wind stress in the south is increased. An additional experiment was run in which the zonal wind stresses north of 30°S were set to zero while the zonal wind stresses south of 30°S were held at the 1.0× levels. The Atlantic outflow in this experiment remains essentially the same as the outflow in the standard model. Thus, in this set of experiments at least, the winds north of 30°S do not contribute much to the large-scale overturning.

Figure 4 shows the Atlantic outflow in 0.5×, 1.0× and 1.5× plotted against the northward Ekman drift at the tip of South America, $\int (\tau_x/f)\mathrm{d}x_{\mathrm{SA}}$. "Atlantic outflow" is determined from the streamfunction diagrams in Fig. 3. It is defined as the southward flow at 30°S which has a North Atlantic origin. When plotted against $\int (\tau_x/f)\mathrm{d}x_{\mathrm{SA}}$, the Atlantic outflow from each model run is part of a quasi-linear trend. If the trend in Fig. 4 is extrapolated to a condition of zero wind stress it predicts an outflow of only 2 Sv. The Atlantic outflow, as defined here, does not include deep water of Antarctic origin which can be seen in the deeper cells in Fig. 3.

Figure 4 also includes results from two paired low-resolution model experiments (MANABE and STOUFFER, 1988; COX, 1989). Two of these results, "Cox Exp. 3" and "Manabe and Stouffer, non-sinking solution", come from models in which surface salinities in the North Atlantic are too low for deep water to form. These results plot along the x axis. There is no Atlantic outflow even though a wind stress is being applied in the

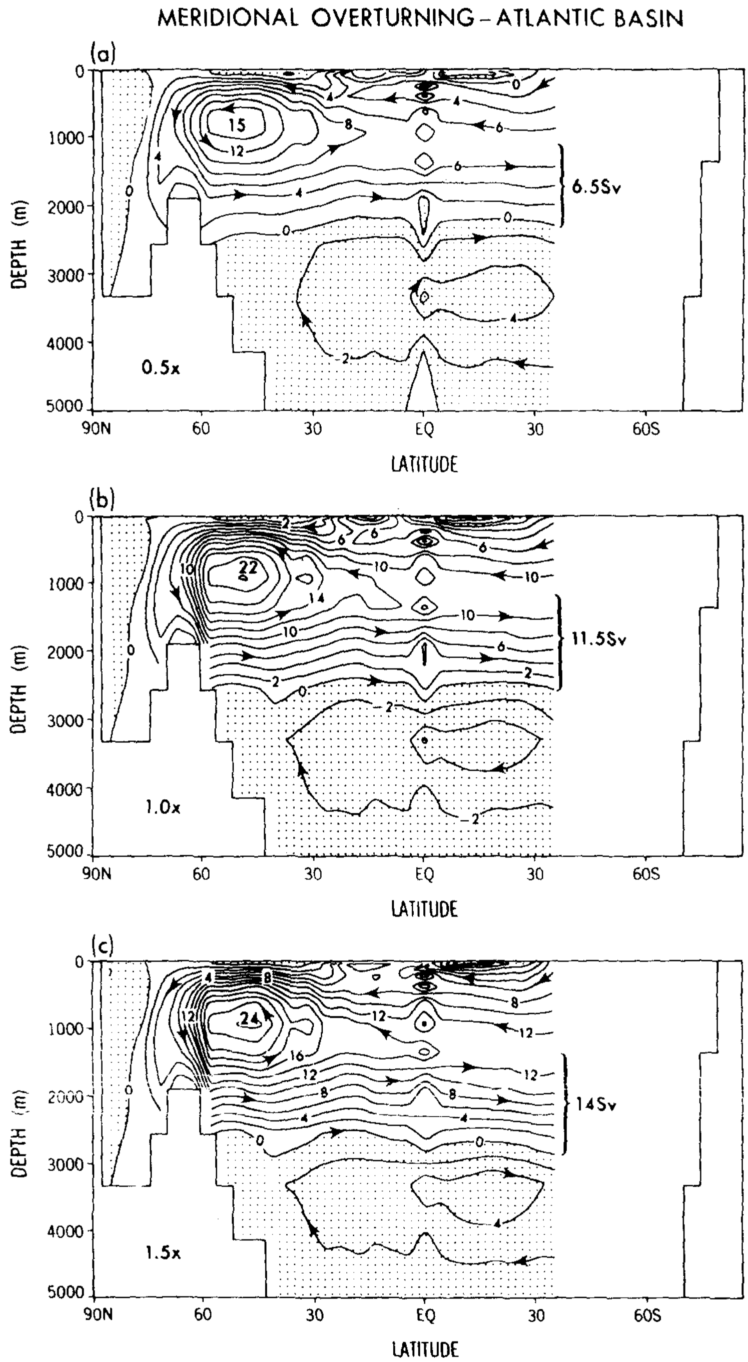

Fig. 3. Meridional overturning in the Atlantic basin from the 0.5× (top), 1.0× (middle) and 1.5× (bottom) wind sensitivity experiments. The flow between stream lines is 2 Sv. The outflow of deep water (of North Atlantic origin) through the South Atlantic scales with the wind stress applied south of 30°S. The model's outflow is indicated by the bracketed streamlines between roughly 1300 and 2600 m.

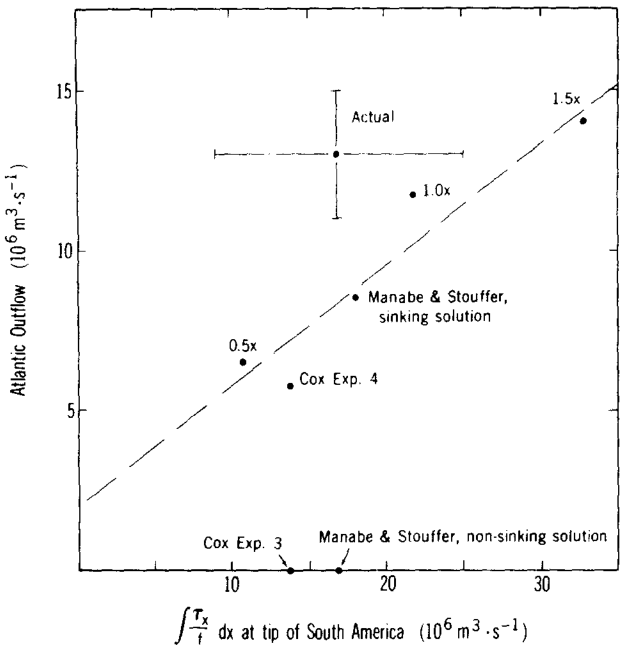

Fig. 4. Atlantic outflow in the 0.5×, 1.0× and 1.5× wind-sensitivity experiments plotted against the zonally integrated Ekman transport at the tip of South America, $\int (\tau_x/f)dx_{SA}$, (units 10^6 m^3 s^{-1}, or Sv). Additional results from similar low-resolution models have been added — "Cox Exp. 3" and "Cox Exp. 4" (Cox, 1989), and "Manabe and Stouffer, sinking" and "Manabe and Stouffer, non-sinking" (MANABE and STOUFFER, 1988). The dashed line across the figure is a regression line linking all non-zero points. An estimate of the actual Atlantic outflow and $\int (\tau_x/f)dx_{SA}$ is given, including error bars.

south. In "Cox Exp. 4" and "Manabe and Stouffer, sinking solution" surface salinities in the North Atlantic are more like those observed and deep water formation occurs. The outflows in the latter two cases plot along the same linear trend as the 0.5×, 1.0× and 1.5× wind experiments.

These paired experiments show that the high salinities of the North Atlantic are necessary for deep water formation and outflow. This is not surprising. But they also suggest that there may be a threshold in the deep water formation/overturning system: once salinities rise to the point that deep water formation can begin, the rate of deep water formation and outflow may "lock on" to the wind-driven removal of deep water in the south.

For reference, Fig. 4 shows the outflow of North Atlantic water actually observed plotted along with the Ekman drift determined from the zonally integrated wind stress at the actual position of Cape Horn. RINTOUL (1991) estimated that the southward flow of deep water across 32°S in the Atlantic basin is 17 ± 4 Sv. Four of the 17 Sv represents a return flow of Antarctic Bottom Water, such that only 13 of the 17 Sv represents water which sank in the North Atlantic.

As pointed out above, the northward Ekman drift given by the HELLERMAN and ROSENSTEIN (1983) climatology for the first row of model grid points south of the tip of

South America is 22 Sv. However, the tip of South America in this particular coarse-resolution model is about 5° north of its actual position. The Ekman transport given by Hellerman and Resenstein at the latitude of the actual tip of South America, 56°S, is about 16–17 Sv. Needless to say, the zonally integrated wind stress at these latitudes is not very well known. In Fig. 4, the observed Ekman drift is plotted as 17 ± 8 Sv. The wind-stress climatology prepared by TRENBERTH *et al.* (1990) suggests that the Ekman drift at these latitudes could be beyond the high end of this range.

"North Atlantic restore" experiments

The density of the North Atlantic Deep Water formed in these model runs is much lower than observed (TOGGWEILER *et al.*, 1989a,b). NADW in the standard 1.0× model tends to be salty enough, but it is several degrees too warm. An additional set of experiments were conducted to see if the density of NADW could have an effect in the variable wind experiments.

The density effect was tested in two ways. First, predicted values of temperature and salinity were restored toward the LEVITUS (1982) data at all levels in the interior north of 46.7°N in each of the 0.5×, 1.0× and 1.5× models. The interior restoring was limited to the North Atlantic and Arctic basins, and a restoring time constant of 1/10 y^{-1} was used. This set of model runs is referred to as the "North Atlantic restore" experiment. The restoring basically cools the deep water in the far North Atlantic by about 2.5°C, which is equivalent to a σ_Θ increase of ~0.25 units. Each of the North Atlantic restore models was run out for ~2000 years as before.

In the second test, the interior restoring was removed, but the surface waters north of 46.7°N in the North Atlantic were cooled by 2.5°C (i.e. T^*, the surface temperatures being restored to, were reduced by 2.5°C). Surface temperatures were not allowed to fall below −1.8°C. This set of model runs is referred to as the "modified North Atlantic T^*" experiment. Each of the modified North Atlantic T^* models was also run out for ~2000 years.

Results of the North Atlantic restore and modified North Atlantic T^* experiments are shown in Fig. 5 using the same format as Fig. 4. In each case the Atlantic outflow for a given amount of wind stress at the tip of South America is larger, but the slope relating to Atlantic outflow with the southern hemisphere wind stress is maintained. Extrapolating the Atlantic outflow to zero winds yields about 10 Sv of outflow vs 2 Sv before.

Making the deep water in the North Atlantic denser does increase the outflow of deep water through the South Atlantic. However, the sensitivity of the outflow to the wind stress seems to remain the same without regard to the manner in which the density increase was obtained. These experiments reinforce a result noted above. A 1.0× wind forcing in the south seems to establish some kind of threshold or baseline outflow of ~10 Sv. The outflow can be increased by making North Atlantic Deep Water denser, but the wind forcing seems to establish a lower limit to the outflow once the North Atlantic is salty enough to allow deep water to form.

At this stage of model development it is difficult to further differentiate the effect of density from the effect of the wind. The model's method of restoring surface temperatures to fixed observed temperatures does not allow for much feedback between a model's overturning and its surface temperature field. Ocean models run without an interactive atmosphere miss important air–sea interaction processes which have a lot to say about how deep water forms.

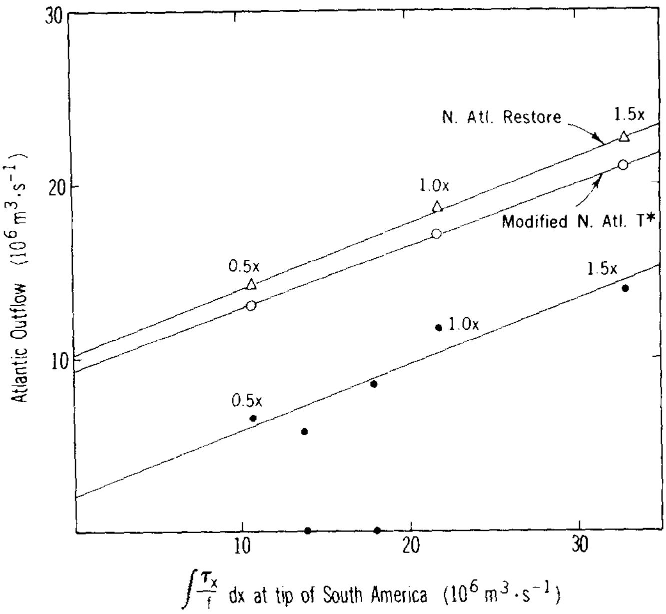

Fig. 5. Atlantic outflow vs $\int (\tau_x/f) dx_{SA}$ in "North Atlantic restore" (open triangles) and "Modified North Atlantic T^*" (open circles). In the North Atlantic Restore experiment, interior temperatures and salinities north of 46.7°N in the North Atlantic are restored toward LEVITUS (1982) observations. The restoring cools interior temperatures north of 46.7°N by an average of about 2.5°C. In the Modified North Atlantic T^* experiment, the surface temperatures being restored *to* (i.e. T^*) are cooled by 2.5°C with respect to annual mean Levitus temperatures. The closed circles show results from Fig. 4 replotted for comparison. Note the scale change in the vertical axis. The increase in density brought about by reducing North Atlantic temperatures increases the Atlantic outflow by some 7–8 Sv. The sensitivity of Atlantic outflow to southern hemisphere winds, as measured by the slope between the various 0.5×, 1.0× and 1.5× versions of the model, is very much the same as it is without interior restoring or surface cooling.

MOMENTUM BALANCE IN THE LATITUDE BAND OF DRAKE PASSAGE

The outflow of deep water from the Atlantic in the standard (1.0×) experiment is 11.5 Sv. This is only half the northward Ekman drift in the first row of grid boxes south of the tip of South America. The 2:1 relationship between the Ekman drift and the Atlantic outflow is reflected in the roughly ~0.5 slope linking these quantities in Figs 4 and 5. This section, illustrates how this relationship is obtained in the model.

The global meridional stream function in Fig. 1 shows that the poleward flow crossing into the latitude band of Drake Passage is concentrated at two depths. About half the poleward flow takes place below the depth of the sill where it can be geostrophically balanced. The poleward flow below the sill is roughly the same as the outflow of deep water from the Atlantic at 30°S. The other half of the poleward flow crossing into the latitude band of Drake Passage occurs in the upper two kilometers where it cannot be geostrophically balanced.

The momentum budget for the flow through Drake Passage is illustrated in Fig. 6 following the procedure of GILL and BRYAN (1971). The volume of ocean between 40° and 70°S has been broken up into eight zonal slabs, each of which is a single grid box wide in the

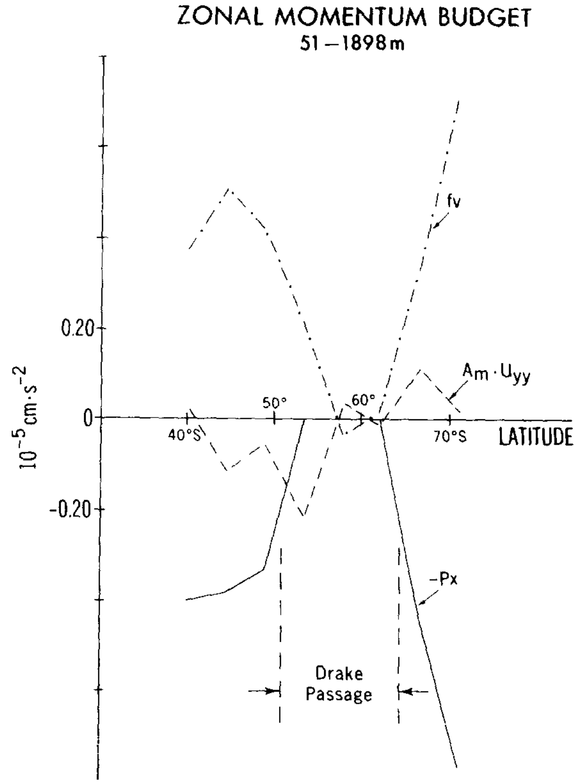

Fig. 6. Zonal momentum budget for eight model grid rows between 40° and 70°S in the 1.0× model. Accelerations in each grid row are averaged around the globe between the base of the Ekman layer (51 m) to the bottom of layer 8 (1898 m). The pressure gradient term goes to zero in the three slabs which pass through Drake Passage.

north–south direction. Each extends around the world between the base of the Ekman layer and a depth of 1898 m. Three of the slabs pass through Drake Passage and encounter no topography. The momentum budget in Fig. 6 plots the acceleration on each slab due to pressure gradient forces ($-P_x$), the Coriolis force (fv), and lateral friction ($A_m \cdot u_{yy}$). Friction in the model is parameterized as a viscous drag on the flow in adjacent grid boxes, literally a diffusion of momentum. The three terms in Fig. 6 are the dominant terms in the model's momentum budget and must sum to zero.

In the zonal slabs north of Drake Passage the pressure difference on either side of South America produces a westward acceleration which balances the eastward acceleration due to the Coriolis force. The resulting flow is poleward and nearly in geostrophic balance. In the three slabs which pass through Drake Passage, the pressure gradient force, as expected, is zero. In the first Drake Passage slab adjacent to South America the Coriolis term is still quite large but it is balanced by a large amount of friction. (About 23% of the total friction occurs when the slab's eastward flow rubs up against land at the tip of South America. The remainder occurs in areas of open water.) In the two Drake Passage slabs closest to Antarctica, the Coriolis term, friction term, and poleward flow are all very small.

Friction decelerates the eastward flow in the slab next to South America and balances the Coriolis force much like the missing pressure gradient force. It allows 8 Sv of poleward flow to come into this slab from the north. Thus, friction allows 36% of the surface Ekman drift in the model to "leak" back to the south at fairly shallow depths. The combination of Atlantic outflow (11.5 Sv) and ACC friction (8 Sv) accounts for 90% of the poleward flow balancing the Ekman drift. It is the leakage of near surface waters back to the south, more than any other factor, which accounts for the particular slope linking the model's Atlantic outflow and the applied circumpolar wind stress in Figs 4 and 5.

The deceleration experienced by model slabs due to lateral friction in the latitude band of Drake Passage, 0.1–0.2 $\times 10^{-5}$ cm s^{-2} (Fig. 6), if multiplied by the mass of the water column feeling the friction, $\sim 2 \times 10^5$ g cm^{-2}, is of the same magnitude as the momentum being added every second by the wind stress. This kind of momentum balance is not what one expects to see in the real world. Thus a strong caveat must be added here with regard to the way momentum is dissipated in low-resolution models. Numerical stability determines the value of the viscosity parameter A_m used in these calculations, not the need to simulate an observed viscosity. The value of A_m used in running the model is 2.5×10^9 cm^2 s^{-1}. This is 250 times larger than the coefficient applied to the mixing of tracers. The value of A_m can generally be reduced by a factor of 5–8 each time model resolution is doubled.

A linkage between circumpolar wind stresses and a model's large-scale overturning should be present, at some level, in every global GCM. It may seem surprising to the reader that this linkage has gone largely unnoticed. ENGLAND (1993, p. 1545) has noticed a similar effect in a closely related model. A special circumstance conspires, perhaps, to make the linkage more noticeable in our model. These results are dictated to a large degree by the fact that the model grid resolves the tip of South America at 51°S rather than 56°S. This puts Drake Passage very close to the latitude of the maximum westerly wind stress. It gives our model the potential to draw 22 Sv of deep water poleward. A model with the tip of South America at 56°S puts Drake Passage further from the maximum westerlies. It would have less Ekman drift at the tip of South America and its deep poleward flow should be weaker by 6 or 7 Sv.

Since friction allows part of the poleward flow to leak back to the south at shallow depths, the amount of deep water actually drawn poleward by the wind stress is reduced. In our example above, this reduction is about 8 Sv. Thus, the effect of friction has the same magnitude, but opposite sign, as the effect of locating the tip of South America north of its real position by 5°. The effect of unrealistic model friction is nearly compensated by the "special circumstance" of unrealistic continents.

The idealized model in Cox (1989) has South America at the right place and only 14 Sv of Ekman drift at the tip of South America. Cox's model has no topographic obstructions to impede its ACC, except a sill in Drake Passage. His wind-forced model has a very strong ACC ($\sim$220 Sv) and friction is a major component in its momentum budget. Cox's model is left with only 6 Sv of deep poleward flow (see TOGGWEILER and SAMUELS, 1993a). The idealized model of MAROTZKE and WILLEBRAND (1991) does not have a sill in its Drake Passage. They have no net poleward geostrophic flow south of their southern hemisphere continents at any depth. The idealized model of HUGHES and WEAVER (1994) has only 8 Sv of Ekman drift at the tip of South America in their standard case (T. HUGHES, personal communication).

All GCMs have a competing variety of overturning in which deep waters sink near the poles and upwell into the thermocline in low and middle latitudes. This type of overturning is facilitated by vertical mixing which warms the interior and allows deep water to be removed upward (see Discussion). In single basin ocean models without Drake Passage or an ACC, this variety of overturning is the only game in town (BRYAN, 1987). The degree to which the Drake Passage effect is apparent in a particular model is obviously a question of how strong the two types of overturning are. A buoyancy-forced overturning will dominate when relatively large coefficients of vertical mixing are employed and the wind stress in the latitude band of Drake Passage is weak. The Drake Passage effect should dominate in the limit of weak vertical mixing, strong circumpolar winds, and limited friction.

DISCUSSION

Mid-depth poleward flow in the high latitudes of the Southern Hemisphere

The idea that the outflow of deep water from the Atlantic might be related to the wind stress in the latitude band of Drake Passage is based largely on an assumption that the poleward flow balancing the Ekman transport in the latitude band of Drake Passage should be deep and geostrophically balanced. How can one evaluate from oceanographic data whether poleward flows in the real world are in fact deep and geostrophically balanced? Is there any evidence that there are shallow poleward flows which are balanced some other way?

Long-standing oceanographic observations are consistent with the idea that a northward moving Ekman layer in the Southern Ocean is balanced by a mid-depth poleward flow. MERZ and WUST (1922) drew a direct connection between a warm, salty, mid-depth water mass in the Atlantic sector of the Southern Ocean with the salty deep water spreading southward from the North Atlantic. DEACON (1937) demonstrated that Merz and Wust's warm, salty water mass, now known as Circumpolar Deep Water, is a continuous feature around Antarctica. He also identified Indian and Pacific contributions to the Circumpolar Deep Water.

Deacon's observations inspired SVERDRUP *et al.*'s (1942) zonally averaged circulation schematic (reproduced here, as Fig. 7). WYRTKI (1961), similarly inspired, outlined a theoretical thermohaline circulation driven by the fields of Ekman convergence and divergence in the circumpolar belt. Wyrtki's scheme has obvious similarities to the idea described here, but Wyrtki did not link the existence of the mid-depth poleward flow to the dynamic effect of Drake Passage.

More recent tracer observations clearly support the idea that surface waters transported out of the Southern Ocean to the north are being replaced by relatively old deep water. Most of the chlorofluorocarbons (CFCs) and bomb ^{14}C observed south of the ACC are found in the near surface layers or in newly formed bottom waters (TRUMBORE *et al.*, 1991; ROETHER *et al.*, 1993; SCHLOSSER *et al.*, 1994). North of the Circumpolar Current, CFCs and bomb ^{14}C are found in fairly high concentrations throughout the upper kilometer. BROECKER *et al.* (1985) show that only 1/3 of the bomb ^{14}C which entered the ocean south of the ACC remained south of the ACC at the time of the GEOSECS surveys. Overall five to six times more bomb ^{14}C is found per unit area north of the ACC even though the rate of input on either side of the ACC is more-or-less the same.

These observations show that the northward transport of water in the Ekman layer carries bomb ^{14}C and the CFCs out of the Southern Ocean immediately after these tracers enter the ocean. The surface waters lost to the north are replaced by upwelled

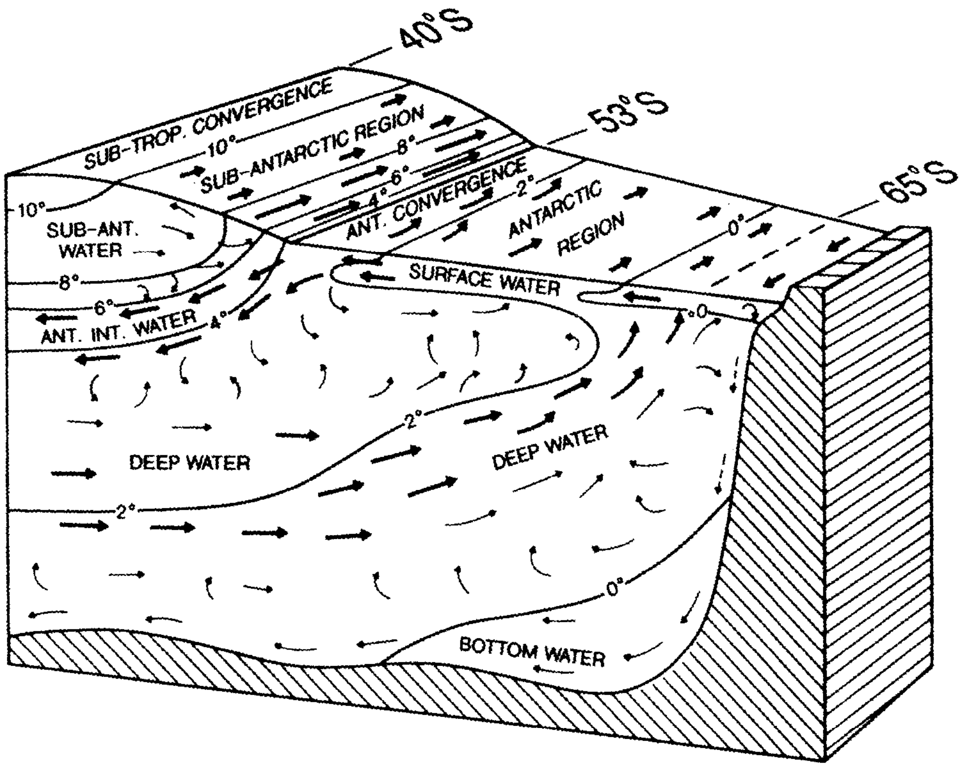

Fig. 7. Schematic of the Southern Ocean showing the meridional circulation inferred from water masses (after SVERDRUP *et al.*, 1942). Arrows tracking the southward flow of deep water have been highlighted. Approximate latitudes have been added to the original figure.

deep water which is largely devoid of bomb ^{14}C and CFCs. At a minimum one can say that the water masses moving northward out of the region are not reconnecting with the deep water masses moving southward over time scales of less than 50 years. In fact, the deep water upwelling around Antarctica has a nominal age of well over 500 years in terms of its natural or pre-bomb ^{14}C content. Thus, it is quite clear that relatively deep water dominates the poleward flow in the southern hemisphere.

It is important to point out that these observations do not make a clear statement about the exact depth at which mid-depth water moves southward into the Southern Ocean. Bomb ^{14}C and CFC observations require that the main poleward flow be below the penetration depth of anthropogenic tracers. Otherwise, they do not point to any particular depth. As pointed out by WARREN (1990), the poleward transport of the salty Atlantic water across the latitude band of Drake Passage appears to be deep enough that it could be constrained by the topography in the latitude band of Drake Passage. Meanwhile, meridional sections of temperature and oxygen in DEACON (1937) and SVERDRUP *et al.* (1942) show continuous temperature maxima and oxygen minima across the circumpolar belt at depths above 1000 m. If these tracer features are indeed associated with poleward flows they are clearly not influenced by the deep topography in the latitude band of Drake Passage.

Basin-by-basin transport across the latitude band of Drake Passage

The Drake Passage effect requires that there be no *net* southward transport of upper kilometer water across the gap between South America and Antarctica. But there can be bi-directional flows across the gap carried by basin-scale geostrophic flows and small-scale eddies. Bi-directional flows can produce a net transport of water properties without a net transport of mass. GORDON *et al.* (1981) describes a huge, deep-reaching cyclonic gyre in the Weddell–Enderby sector of the Southern Ocean which cuts right across the latitude band of Drake Passage. The ACC itself moves large volumes of water into and out of the latitude band of Drake Passage as it is deflected by bottom topography and continental obstructions.

Figure 8 shows a basin-by-basin breakdown of the meridional circulation in the standard 1.0× model. Instead of showing the meridional circulation as a stream function, which cannot be meaningfully integrated in single basins south of Africa or Australia, this set of figures shows the mean circulation by vectors which represent the zonally averaged v and w components flow. We have eliminated the arrows in the surface layer Ekman layer, which would otherwise be very large in relation to the arrows shown here.

Meridional flows within the Indian (Fig. 8a), Pacific (Fig. 8b), and Atlantic (Fig. 8c), show no obvious restrictions in the latitude band of Drake Passage. One sees a strong southward component to the flow in the Indian Ocean associated with the southward displacement of the ACC. There is a convergence in the Pacific where water leaves the basin via Drake Passage, and a corresponding divergence in the Atlantic where the ACC flows into the basin and turns northward. For the most part, these are all geostrophically balanced flows.

It is only the meridional circulation averaged around whole latitude circles (Fig. 8d), that looks like the global stream function in Fig. 1. The average v, w flow in latitude band passing through Drake Passage is nearly vertical. In the first row of grid boxes south of the tip of South America the vectors in the upper kilometer have a slight poleward component. This represents the frictionally supported flow illustrated in Fig. 6. The model's nearly vertical net flow in Fig. 8d does not look anything like the circulation schematic constructed by SVERDRUP *et al.* (1942) in Fig. 7. The vertical net flow is a very robust feature in ocean circulation models, even in models with much higher resolution than the model used here (SEMTNER and CHERVIN, 1992; DÖÖS and WEBB, 1994).

The vectors tracking the poleward and upward flow in the vicinity of Drake Passage seem to connect with vectors tracking downward flows immediately north of Drake Passage. This is a feature seen prominently in GCM stream function diagrams (Fig. 1). The downward motions north of Drake Passage seem to combine with the northward flow in the surface Ekman layer and upward motions within the latitude band of Drake Passage to form a closed overturning cell. Modellers often call this closed feature the "Deacon Cell". The downward motions associated with the Deacon Cell is not a feature that one would infer from tracer observations. The downwelling north of Drake Passage and the closed nature of the overturning in this region can be quite misleading (see Appendix).

Spreading of tracers across the latitudinal band of Drake Passage

DEACON (1937) and SVERDRUP *et al.* (1942) claimed to see a net mid-depth poleward flow into the Southern Ocean from the spreading of tracers. Since some of this spreading activity occurs at depths well above the depths where a net geostrophic flow is allowed, it

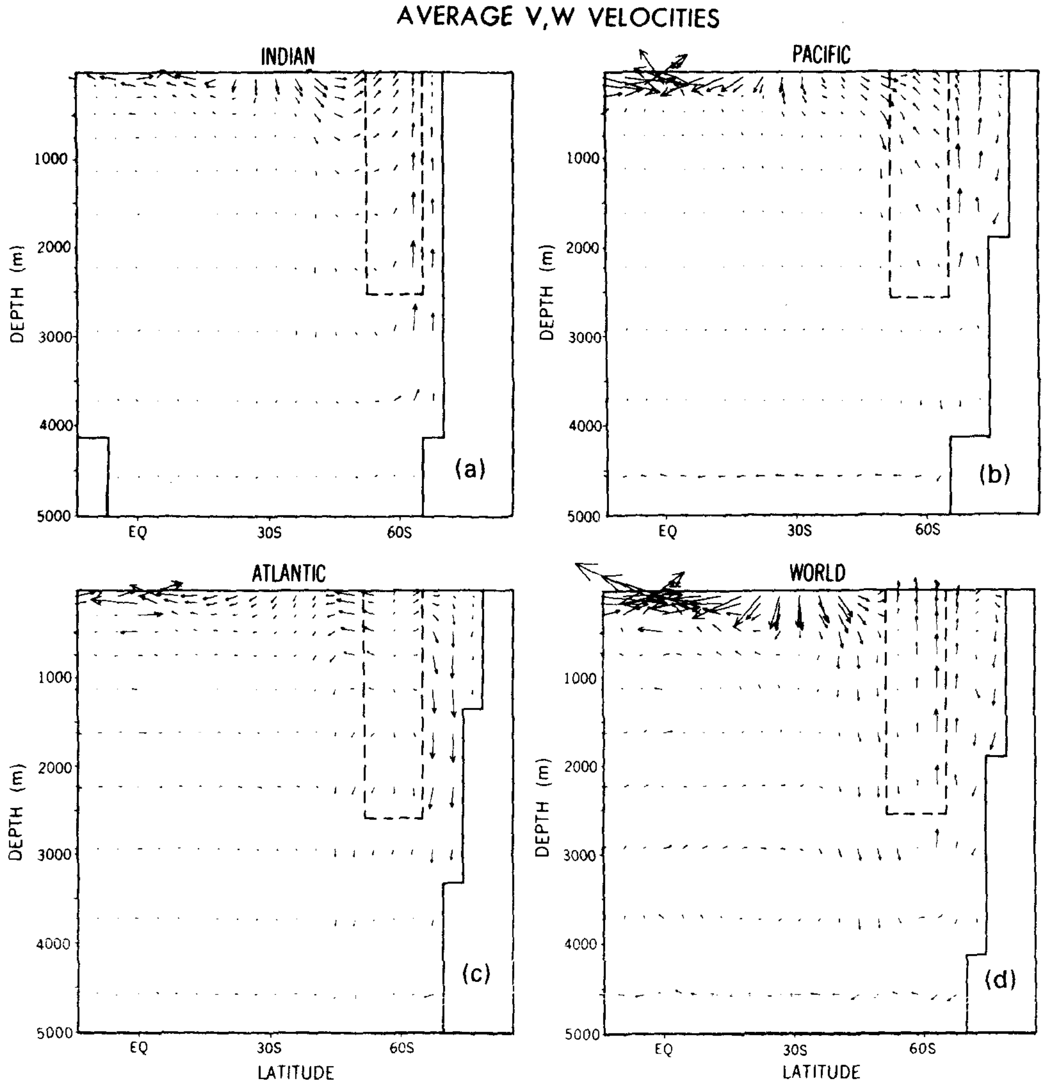

Fig. 8. Basin-by-basin, v, w velocities averaged in the zonal direction over the southern hemisphere in the 1.0× model. Panel (a) shows v, w velocities for the Indian Ocean, (b) Pacific, (c) Atlantic and (d) World. Boxes centred on 60°S indicate the depth and latitudinal extent of Drake Passage. The length of each vector has been scaled by the length of a latitude circle in each grid row and in each basin.

could be cited as evidence that the ocean does not feel the Drake Passage constraint as much as is claimed here. It must be pointed out that many of the tracer features which inspired Deacon and Sverdrup *et al.*'s circulation schematics are found in only part of the Southern Ocean. They are not necessarily representative of the zonal mean flow. This section will show that the bi-directional flows illustrated in Fig. 8 can move tracers quite readily across the latitude band of Drake Passage even though a net poleward flow is inhibited. This makes the Drake Passage effect hard to document, or to refute, in tracer distributions.

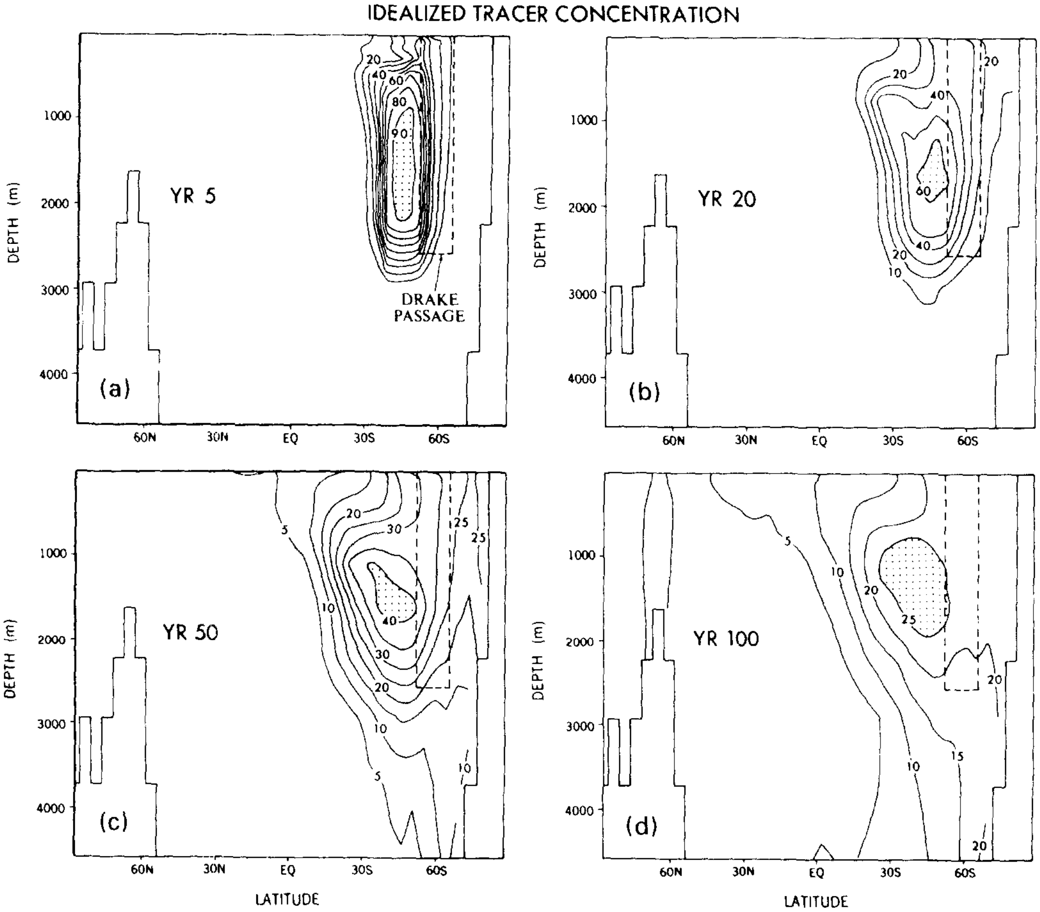

Fig. 9. Results of an idealized tracer experiment in which a numerical dye is released in a mid-depth zonal strip just north of Drake Passage. The figure shows tracer concentrations averaged in the zonal direction 5 years (a), 20 years (b), 50 years (c), and 100 years (d) after the tracer release. Initial tracer concentration is 100 units. Box centered on 60°S indicates the position of Drake Passage.

In one example, an idealized numerical tracer was released into a zonal strip around the whole globe just north of the latitude band containing Drake Passage, 37°S–51°S. The vertical extent of the tracer release was 483–2228 m (model levels 5–9). Numerical values of the tracer were continuously restored to 100 units within the strip for a duration of two years. After two years, the restoring was turned off. A no-flux boundary condition was maintained at the surface everywhere and at all times.

Figure 9 shows the latitudinal distribution of the tracer, averaged around the globe, at the end of years 5, 20, 50 and 100. By year 5, the tracer has not moved much in the north–south direction, but it has penetrated vertically to the surface, especially at 51°S. By year 20, the tracer has moved southward across the latitude band of Drake Passage. A lobe of high-tracer water is beginning to penetrate northward near 750 m. This lobe traces water being carried northward by the overturning cell in the Atlantic basin. At this stage, the overall meridional spreading of the tracer field is not much greater than one would expect from the model's parameterized lateral diffusion. By year 50, the tracer has spread much more widely than one would expect from simple diffusion. The tracer patch has reached Antarctica and has penetrated vertically into the bottom water. By year 100, the tracer is nearly homogenized south of 60°S.

The zonal strip into which the tracer was released contains most of the ACC. Mean eastward velocities in the middle of the zonal strip are about 2 cm s^{-1}. Thus one circumnavigation of the globe takes about 30 years. The dispersal of the tracer field reflects this consideration. By year 50, the individual tracer "particles" have had a chance to circumnavigate the globe. They have encountered the full range of bi-directional flow and the effect of vertical convection near Antarctica.

In the 50-year panel of Fig. 9 one sees an indication of upward penetration by low-tracer water south of Drake Passage. Low-tracer water appears to have worked through the tracer patch as part of a geostrophically balanced flow below the sill between South America and Antarctica. This is the only clear indication of the Drake Passage effect in this experiment. By year 100, the Drake Passage effect is not nearly so obvious.

In a second example, the northward moving Ekman layer in the latitude band of Drake Passage was tagged. Tracer concentrations were set to 100 units in the model's surface layer over in a zonal strip between 51°S and 65°S for a duration of two years. A no-flux surface boundary condition was maintained everywhere else. At the end of two years the surface boundary condition between 51°S and 65°S reverts to no-flux.

Figure 10 shows the zonal mean distribution of the tracer at the end of years 2, 10, 20 and 50. By the end of year 2, the tracer has penetrated below 1000 m, mainly by convection. By year 10, there is some net northward movement near the surface, and a fairly strong downward penetration below 2000 m adjacent to Antarctica. By year 20, the tracer is just reaching the equator near the surface, but has reached the bottom in fairly high concentrations around Antarctica. At year 20, one sees a strong southward penetration of low-tracer water below the sill which extends upward in the region south of Drake Passage. By year 50, the signature of poleward flow below the sill has been largely wiped out as the tracer becomes more vertically homogenized.

By year 150 (Fig. 11) the entire Atlantic basin has been nearly filled with tracer. The tracer has traversed the length of the basin near the surface and become incorporated into North Atlantic Deep Water. The tracer has also penetrated into the northern hemisphere at the bottom. Given the starting distribution, there is a surprisingly small preference for the tracer to be in the upper part of the Atlantic overturning cell vs the Antarctic cell at the bottom. This is testimony to the power of convection in the initial stages of tracer dispersal. Even though the vertical flow in the latitude band of the tracer's release is strongly upward, and even though the Ekman layer initially moves the tracer patch northward, convection moves the tracer downward even faster.

One could perform hundreds of similar experiments with the ocean model. What one would find is that the restrictions on net meridional flows imposed by Drake Passage is not readily apparent in tracer fields. Convection, diffusion and bi-directional flows obscure the effect. Details about where a tracer is introduced, how it is modified at the surface or in the interior, and the length of time between tracer introduction and observation, have an important bearing on whether or not the Drake Passage effect can be seen.

The existence of the Drake Passage effect is ultimately dependent only on the net transport of mass integrated over whole latitude circles, not the transport or spreading of

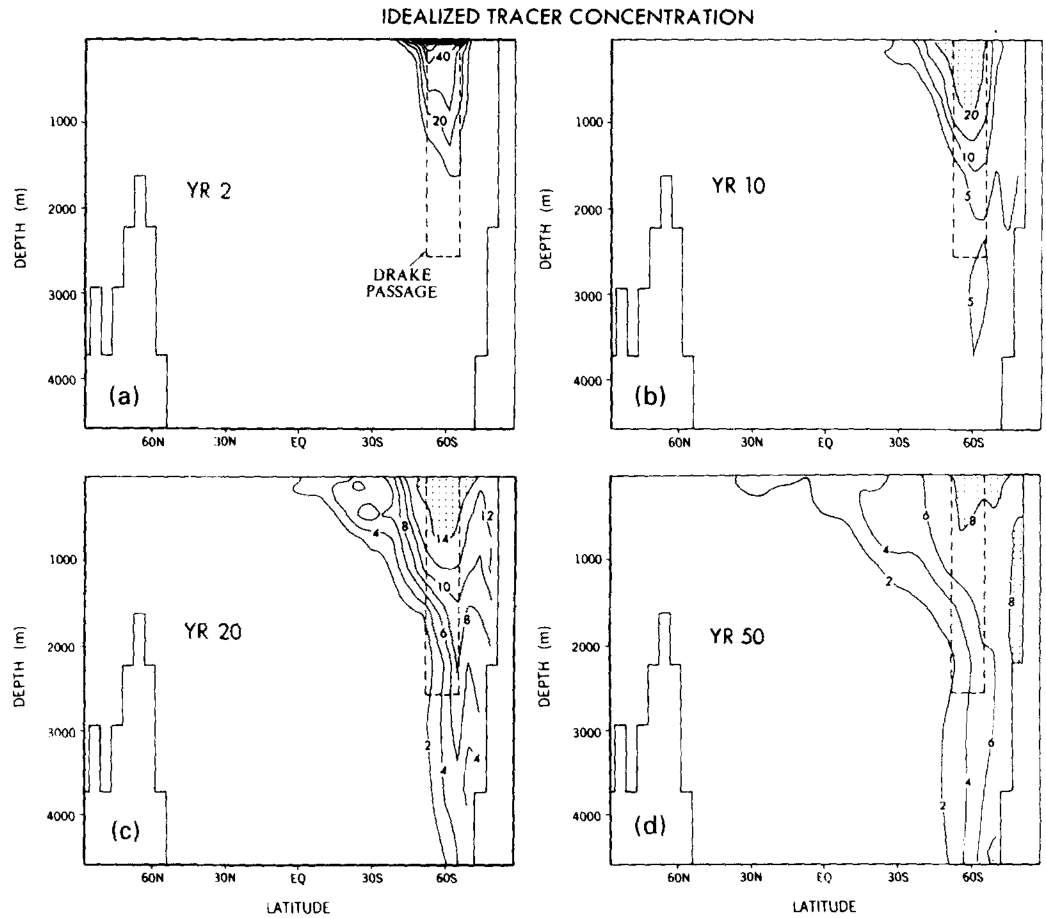

Fig. 10. Results of an idealized tracer experiment in which a numerical dye is released in the 1.0× model's surface layer in a zonal strip between 51° and 65°S. Figure shows tracer concentrations averaged in the zonal direction 2 years (a), 10 years (b), 20 years (c), and 50 years (d) after the tracer release. Initial tracer concentrations is 100 units. Box centered on 60°S shows the location of Drake Passage

tracers. No inconsistency can be seen between the tracer spreading identified by Deacon and Sverdrup *et al.* and the net mass flow produced by ocean models. An exception is made for one important feature, however, see the Appendix.

Need for a new idea

Existing descriptions of the ocean's thermohaline circulation generally invoke a scenario in which the ocean's deep and bottom waters are removed upward into the thermocline. STOMMEL (1958) describes the thermocline as a "pump" which removes deep water upward as heat is mixed or stirred downward. Some kind of vertical mixing, equivalent to a Fickian diffusion of O(1 cm^2 s^{-1}), supposedly warms the ocean's deep water, making it buoyant with respect to newly formed bottom waters. In the model of

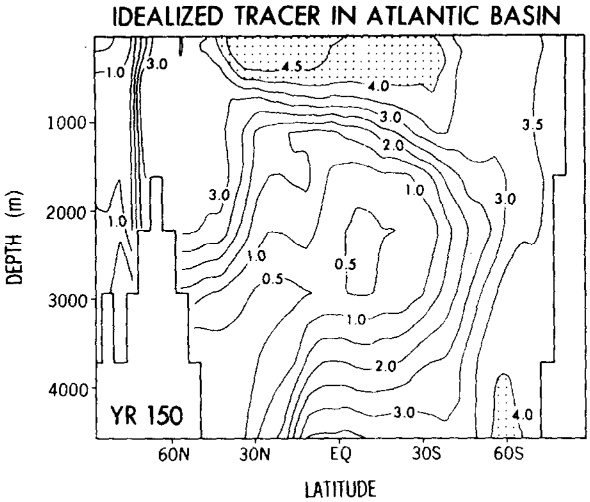

Fig. 11. Idealized tracer distribution in the Atlantic basin 150 years after tracer release from the experiment illustrated in Fig. 10 (surface-layer release).

STOMMEL and ARONS (1960), new deep water sinks and flows away from the polar regions in response to the upward removal of deep water via the thermocline pump.

The upwelling needed to remove ~20 Sv of deep water over the area of the ocean's thermocline amounts to some 2–3 m y^{-1}. This cannot be directly measured. Oceanographers have tried instead to determine whether enough vertical mixing exists to sustain this level of upwelling. Actual mixing rates seem to be at least an order of magnitude lower than necessary (GARRETT, 1979; LEDWELL *et al.*, 1993). This implies that the quantity of deep water removed by upwelling in low and middle latitudes may be more like 2 Sv, rather than 20 Sv. In the scenario described here, new deep water sinking in the North Atlantic upwells around Antarctica where the process is directly forced by the wind and can actually be observed. This kind of overturning can remove 15–20 Sv from the interior of the ocean without any requirement for O(1 cm^2 s^{-1}) vertical mixing.

BROECKER (1991) and GORDON (1986) have popularized the notion that the Atlantic overturning is part of a "Great Conveyor" which is spread across the Atlantic, Indian and Pacific Oceans. They suggest that the conveyor is mainly driven by a build up of salt in the North Atlantic. According to this point of view, the Atlantic outflow is driven by a north–south density contrast created when the North Atlantic's salty surface water is cooled in high northern latitudes.

A very pertinent question is whether the build up of salt in the North Atlantic actually drives 15–20 Sv of deep water out of the Atlantic. Broecker and Gordon do not at any point quantify a relationship between a particular north–south density contrast and a particular level of outflow. It is important to remember that east–west pressure gradients along the length of the Atlantic basin, not the north–south density contrast, ultimately sustain the Atlantic's outflow (WARREN, 1981).

The back end of the Great Conveyor functions much like the thermocline in the Stommel/Arons scheme. The formation of new deep water in the North Atlantic is supposedly balanced by upwelling in the Indian and Pacific Oceans. Vertical mixing must be invoked to warm and freshen old NADW in order that buoyancy forces can remove it upward. It would be simpler to think of the Great Conveyor as an Atlantic–Antarctic system in which the mass of deep water flowing out of the Atlantic upwells entirely around Antarctica. The salt associated with NADW is free to mix and spread into the Indian and Pacific basins as observed, but the mass associated with the outflow from the Atlantic does not have to upwell there.

The "North Atlantic restore" results in this paper show that an increase in the density of North Atlantic deep water can be translated into steeper east–west pressure gradients and a stronger outflow. But southern hemisphere winds do this too. The model results in this paper suggest that southern hemisphere winds establish a base level of outflow which may account for most of the total outflow. It is acknowledged that some degree of salinification is necessary to allow deep water formation to begin, but the build up of salt may not account for the volume of outflow or its stability over time.

CONCLUSIONS

The quantity of deep water flowing out of the Atlantic basin is similar to the quantity of deep water removed from the interior of the ocean by the Ekman divergence around Antarctica. Model sensitivity tests in this paper suggest that this is no coincidence. In our model, the removal of deep water by the winds around Antarctica induces stronger outflows of deep water in the South Atlantic and more deep water formation in the North Atlantic. The key to this linkage is the prohibition on any net geostrophically balanced poleward flow in the latitude band containing Drake Passage. Water forced northward as part of the surface Ekman layer can only be balanced by deep water flowing poleward at depths where there is a sill or topographic ridges to support east–west pressure gradients. This enforced separation between equatorward flows at the surface and poleward flows at depth leads to an overturning of the deep ocean which is independent of the vertical mixing and deep upwelling into the thermocline.

Tracer observations are consistent with the mechanism proposed here. Water transported northward out of the Southern Ocean via the surface Ekman layer is replaced by old deep water. The upwelled deep water contains a large component of salty North Atlantic water and is nearly devoid of anthropogenic tracers. It is important to remember that only the *net* transport of deep water into the Southern Ocean is limited by the Drake Passage constraint. Basin-scale geostrophic flows and eddies can transport water properties and tracers across the circumpolar belt even though the net flow is limited.

The Drake Passage effect demonstrated here is probably an unrecognized component of the overturning in every global GCM ever run. The level at which the Drake Passage effect is felt depends on the wind-stress climatology being used and the placement of South America relative to the wind-stress maximum. In the experiments described here, lateral friction also plays an important role, both in the Drake Passage effect itself and also in the overall momentum balance of the Antarctic Circumpolar Current. Thus, one must consider these results with some caution. It remains to be seen whether the Drake Passage effect is robust at higher resolution.

Acknowledgements—The results of the 0.5×, 1.0× and 1.5×, wind sensitivity experiments (Figs 2–4) were first presented at a NATO Advanced Study Institute on the Global Carbon Cycle in September of 1991. These results were initially described in TOGGWEILER and SAMUELS (1993a,b). Much of the experimental work in this paper, including the North Atlantic restore experiments, the momentum budget, and the idealized tracer experiments, was done after the NATO paper was written. We would like to take this opportunity to acknowledge the help we received in producing both this paper and the NATO paper.

None of these model experiments could have been carried out without the pioneering work of Mike Cox, who died in 1989 after a long bout with cancer. Not only did Mike play a major role in developing the GFDL ocean model, but his idealized model experiments (published as Cox, 1989) were the starting point for these investigations. We would like to acknowledge very careful and helpful reviews of the NATO paper by Bruce Warren, Arnold Gordon, Kirk Bryan and Jorge Sarmiento. Don Olson helped make us aware of some of the critical literature on the Drake Passage constraint. We would like to thank Kirk Bryan and Bruce Warren for their reviews of this paper and for their encouragement through the whole process.

REFERENCES

BROECKER W. S. (1991) The Great Ocean Conveyor. *Oceanography*, **4**, 79–89.

BROECKER W. S., T.-H. PENG, H. G. OSTLUND and M. STUIVER (1985) The distribution of bomb radiocarbon in the ocean. *Journal of Geophysical Research*, **90**, 6953–6970.

BRYAN F. (1987) Parameter sensitivity of primitive equation ocean general circulation models. *Journal Physical Oceanography*, **17**, 970–985.

BRYAN K. and L. J. LEWIS (1979) A water mass model of the World Ocean. *Journal of Geophysical Research*, **84**, 2503–2517.

COX M. D. (1989) An idealized model of the world ocean. Part 1: The global-scale water masses. *Journal of Physical Oceanography*, **19**, 1730–1752.

DEACON G. E. R. (1937) The hydrology of the Southern Ocean. *Discovery Reports*, **15**, 1–124.

DÖÖS K. and D. J. WEBB (1994) The Deacon Cell and other meridional cells of the Southern Ocean. *Journal of Physical Oceanography*, **24**, 429–442.

DE SZOEKE R. A. and M. D. LEVINE (1981) The advective flux of heat by mean geostrophic motions in the Southern Ocean. *Deep-Sea Research*, **28**, 1057–1085.

ENGLAND M. H. (1993) Representing the global-scale water masses in ocean general circulation models. *Journal of Physical Oceanography*, **23**, 1523–1552.

GARRET C. (1979) Mixing in the ocean interior. *Dynamics of Atmospheres and Oceans*, **3**, 239–265.

GILL A. E. and K. BRYAN (1971) Effects of geometry on the circulation of a three-dimensional southern hemisphere ocean model. *Deep-Sea Research*, **18**, 685–721.

GORDON A. L., D. G. MARTINSON and H. W. TAYLOR (1981) The wind-driven circulation in the Weddell–Enderby Basin. *Deep-Sea Research*, **28**, 151–163.

GORDON A. L. (1986) Interocean exchange of thermocline water. *Journal of Geophysical Research*, **91**, 5037–5046.

HELLERMAN S. and M. ROSENSTEIN (1983) Normal monthly wind stress over the world ocean with error estimates. *Journal of Physical Oceanography*, **13**, 1093–1104.

HUGHES T. M. and A. J. WEAVER (1994) Multiple equilibria of an asymmetric two-basin ocean model. *Journal of Physical Oceanography*, **24**, 619–637.

LEDWELL J. R., A. J. WATSON and C. S. LAW (1993) Evidence for slow mixing across the pycnocline from an open-ocean tracer-release experiment. *Nature*, **364**, 701–703.

LEVITUS S (1982) *Climatological atlas of the world ocean*. NOAA Professional Report 13, U.S. Government Printing Office, Washington, D.C.

MANABE S. and R. J. STOUFFER (1988) Two stable equilibria of a coupled ocean–atmosphere model. *Journal of Climate* 1, 841–866.

MAROTZKE J. and J. WILLEBRAND (1991) Multiple equilibria of the global thermohaline circulation. *Journal Physical Oceanography*, **21**, 1372–1385.

MERZ A. and G. WUST (1922) Die atlantische Vertikalzirkulation. *Zeitscrift der Gesellshaft fur Erdkunde zu Berlin*, Jahrgang 1922, 1–35.

MUNK W. H. and E. PALMEN (1951) Note on the dynamics of the Antarctic Circumpolar Current. *Tellus*, **3**, 53–55.

PACANOWSKI R., K. DIXON and A. ROSATI (1991) The GFDL Modular Ocean Model Users Guide, Version 1.0, GFDL Ocean Group Tech. Rep. No. 2, Geophysical Fluid Dynamics Laboratory/NOAA, Princeton University, Princeton, N.J. 08542.

RINTOUL S. R. (1991) South Atlantic interbasin exchange. *Journal of Geophysical Research*. **96**. 2675–2692.

ROETHER W., R. SCHLITZER, A. PUTZKA, P. BEINING and K. BULSIEWICZ (1993) A chlorofluoromethane and hydrographic section across Drake Passage: deep water ventilation and meridional property transport. *Journal of Geophysical Research*, **98**, 14423–14435.

SCHLOSSER P., B. KROMER, R. WEPPERNIG, H. H. LOOSLI, R. BAYER, G. BONANI and M. SUTER (1994) The distribution of ^{14}C and ^{39}Ar in the Weddell Sea. *Journal of Geophysical Research*, **99**, 10275–10287.

SEMTNER A. J. and R. M. CHERVIN (1992) Ocean general circulation from a global eddy-resolving model. *Journal of Geophysical Research*, **97**, 5493–5550.

STOMMEL H. (1958) The abyssal circulation, *Deep-Sea Research*, **5**, 80–82.

STOMMEL H. and A. B. ARONS (1960) On the abyssal circulation of the world ocean — II, an idealized model of the circulation and amplitude in oceanic basins. *Deep-Sea Research*, **6**, 217–233.

SVERDRUP H. U., M. W. JOHNSON and R. H. FLEMING (1942) *The Oceans: their physics, chemistry and general biology*. Prentice-Hall, Englewood Cliffs, New Jersey, 1087 pp.

TOGGWEILER J. R., K. DIXON and K. BRYAN (1989a) Simulations of radiocarbon in a coarse-resolution world ocean model, 1, steady state prebomb distribution. *Journal of Geophysical Research*, **94**, 8217–8242.

TOGGWEILER J. R., K. DIXON and K. BRYAN (1986b) Simulations of radiocarbon in a coarse-resolution world ocean model, 2, distributions of bomb-produced carbon 14, *Journal of Geophysical Research*, **94**, 8243–8264.

TOGGWEILER J. R. and B. SAMUELS (1993a) Is the magnitude of the deep outflow from the Atlantic Ocean actually governed by southern hemisphere winds? In: *The global carbon cycle*, M. HEIMANN, editor, NATO ASI Series, Springer-Verlag, Berlin, pp. 303–331.

TOGGWEILER J. R. and B. SAMUELS (1993b) New radiocarbon constraints on the upwelling of abyssal water to the ocean's surface. In: *The global carbon cycle*, M. HEIMANN, editor, NATO ASI Series, Springer-Verlag, Berlin, pp. 333–366.

TRENBERTH K. E., W. G. LARGE and J. G. OLSON (1990) The mean annual cycle in global ocean wind stress. *Journal of Physical Oceanography*, **20**, 1742–1760.

TRUMBORE S. E., S. S. JACOBS and W. M. SMETHIE (1991) Chlorofluorocarbon evidence for rapid ventilation of the Ross Sea. *Deep-Sea Research*, **38**, 845–870.

WARREN B. A. (1981) Deep circulation of the world ocean. In: *Evolution of physical oceanography scientific surveys in honor of Henry Stommel*, B. A. WARREN and C. WUNSCH, editors, MIT Press, Cambridge, Massachusetts, pp. 6–41.

WARREN B. A. (1990) Suppression of deep oxygen concentrations by Drake Passage. *Deep-Sea Research*, **37**, 1899–1907.

WYRTKI K. (1961) The thermohaline circulation in relation to the general circulation in the oceans. *Deep-Sea Research*, **8**, 39–64.

APPENDIX: DEEP DOWNWELLING AND THE "DEACON CELL"

Global stream function diagrams produced by ocean GCMs, like Fig. 1, define a closed overturning cell in the vicinity of Drake Passage. The closed overturning cell is often referred to by modellers as the "Deacon Cell". The closed nature of this cell suggests that deep downward motions north of Drake Passage are mechanistically connected with the wind-driven upwelling south of the latitude of maximum westerlies and the northward Ekman drift in the surface layer. Given the Drake Passage constraint on net meridional flow (Fig. 8), the existence of a deep upwelling branch in the Deacon Cell makes sense. But what are we to make of the downwelling branch? Ocean observations show that near-surface properties in the 45°–55°S latitude band do not extend much below 1000 m, i.e. below the Antarctic Intermediate Water. It is ironic, given the name applied to this feature, that DEACON (1937) and SVERDRUP *et al.* (1942) did not identify any features that track downwelling to depths of 2000 m and below (Fig. 7).

In viewing a stream function diagram like Fig. 1, it is all too easy to view the deep downwelling north of Drake Passage as a wind-driven feature associated with Ekman transport in the circumpolar belt. However, as we have shown, the sources for the 22 Sv of wind-forced upwelling south of the tip of South America are nearly all accounted for by 11.5 Sv of deep outflow from the South Atlantic and 8 Sv of shallow frictionally balanced poleward flow. There is no sense in our analysis that the upwelling south of the tip of South America is fed by a wind-forced downwelling across 2000 m north of Drake Passage.

GCMs without any wind forcing at all typically produce 10–15 Sv of deep downwelling immediately north of Drake Passage (see Fig. 5 in Cox, 1989; or Fig. 1 in TOGGWEILER and SAMUELS, 1993a). In these models, the downwelling north of Drake Passage is part of a buoyancy-forced circulation linked to upwelling in low and middle latitudes. Because of the constraint on geostrophically balanced flows in the latitude band of Drake

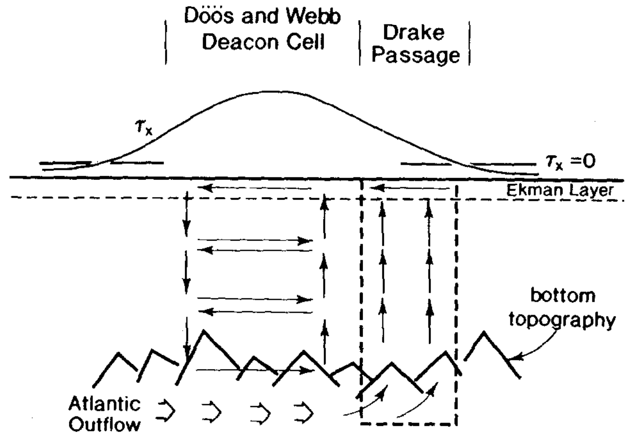

Fig. A1. Schematic diagram of the meridional overturning in the latitude band of the Antarctic Circumpolar Current (ACC) as realized in the high-resolution FRAM model (Döös and Webb, 1994). Döös and Webb's "Deacon Cell" is located north of Drake Passage under the strongest westerly winds. It consists of a number of meridional cells stacked vertically on top of one another. Poleward motions in one cell cancel equatorward motions in the cell just below, leading to the appearance of a large closed cell (the "Deacon Cell") in a zonally integrated stream function. Döös and Webb's Deacon Cell extends vertically to the tops of the topographic ridges which span this latitude band (e.g. Kerguelen Plateau). The Coriolis force associated with the net poleward flow at the bottom of the deepest meridional cell is balanced by pressure gradient forces built against the topographic ridges. In this way, momentum put into the ACC by the wind is ultimately deposited into the solid earth. The individual meridional cells circulate water which is nearly all of the same density such that water properties from the cell nearest the surface are not transferred to the cells below. Water upwelling within Drake Passage (i.e. beyond the tip of South America) has a deeper source which can be related in terms of density to the outflow of deep water from the Atlantic.

Passage, this sort of overturning cannot extend poleward to Antarctica (Gill and Bryan, 1971). The sinking which balances upwelling in low and middle latitudes must be north of Drake Passage. It can be argued that the deep downwelling which closes the Deacon Cell in Fig. 1 is mainly a consequence of this kind of buoyancy-forced circulation.

Direct wind-forced downwelling north of Drake Passage can occur if sinking in the North Atlantic is prohibited or limited in some way. This situation is easy to identify in the momentum balance of the ACC. To illustrate this point a "non-sinking" solution was generated as a variation on the "Modified North Atlantic T^*" series in this paper (Table 1). Instead of enhancing the formation of North Atlantic Deep Water by cooling, we eliminated deep water formation with a fresh water lid.

Northward flows in the surface Ekman layer of the ACC must be balanced by a subsurface poleward subsurface flow. Munk and Palmen (1951) suggested that a deep poleward flow interacting with the bottom topography acts to transfer momentum added to the ACC by the wind into the solid earth. This effect is illustrated very nicely by the non-sinking solution. Elimination of the Atlantic outflow weakens the deep poleward flow in the latitude band of Drake Passage. One anticipates from the argument of Munk and Palmen that the ACC should accelerate, which it does, from 185 Sv to 227 Sv. As the deep outflow from the Atlantic is weakened, more of the momentum added to the ACC by the wind is taken up by friction. The ACC in the non-sinking solution (227 Sv) is as strong as the ACC in the standard model with 1.5× winds (229 Sv). The non-sinking model maintains a deep poleward flow below the depth of the sill in Drake Passage, but in this case the deep poleward flow has an origin in the downwelling north of Drake Passage.

Döös and Webb (1994) have analysed the meridional overturning in the Southern Ocean in the Fine Resolution Antarctic Model (FRAM). Döös and Webb identify an overturning feature which they call the "Deacon Cell" which is superficially similar to the Deacon Cell in our low-resolution model (Fig. 1). In one respect, the FRAM Deacon Cell functions somewhat like the Deacon Cell in our non-sinking solution: it downwells water to depth north of Drake Passage and transfers momentum from the surface Ekman layer into the bottom topography.

In two important respects, the FRAM Deacon Cell is very different. These differences are illustrated in Fig. A1. Downwelling in the FRAM Deacon Cell does not move surface water to depth. The overturning is divided between a number of meridional cells spread along the circumpolar belt, none of which has a vertical excursion of more than a few hundred meters. These cells transfer momentum downward from one to another, but each tends to circulate water which is nearly all of the same density. Thus, the overturning in the FRAM Deacon Cell does not transport mass across isopycnals (DÖÖS and WEBB, 1994). The deep downwelling in our low-resolution model is aided by horizontal mixing which allows the relatively warm water north of Drake Passage to give up heat to the colder water south of the ACC. Mixing allows the downwelling in our low-resolution model to move upper ocean water with near-surface properties across isopycnals.

Whereas the Deacon Cell in our low-resolution model straddles the whole latitudinal extent of the circumpolar westerlies, the Deacon Cell in the FRAM model is located almost entirely north of Drake Passage. This is also illustrated in Fig. A1. The downward transfer of momentum in the FRAM Deacon Cell is concentrated at latitudes where the momentum input from the wind and the ACC are strongest (i.e. 40°–55°S). The vertical extend of the FRAM Deacon Cell north of Drake Passage is set by the height of topographic ridges across this latitude band which help decelerate the ACC by sustaining deep poleward currents. One does not see this feature in low-resolution models mainly because low-resolution models do not resolve these ridges very well. Unable to "feel" the bottom as easily, the ACC simply speeds up until there is sufficient friction to balance the momentum input.

The overturning feature in FRAM which extends into the latitude band of Drake Passage is given by separate identity by Döös and Webb. They call this feature the "Subpolar Cell". The upwelling branch of the Subpolar Cell occurs mainly south of the tip of South America. The upwelling comes from depths between 1600 and 3000 m where its poleward flow in the latitude band of Drake Passage can be geostrophically balanced. Döös and Webb identify the density of the water mass being upwelled as that of North Atlantic Deep Water. Döös and Webb's Subpolar Cell embodies the argument of WARREN (1990) and the Drake Passage effect described in this paper. The term "Deacon Cell" should probably be reserved for the density conserving feature north of Drake Passage.

The deep closed overturning cell in stream function diagrams from low-resolution models is misleading and unrealistic in several ways. Some of the downwelling north of Drake Passage in low-resolution models is part of a buoyancy-driven overturning which is tied to deep upwelling in low and middle latitudes. The downwelling of upper ocean water is made possibly by artificial friction and artificial mixing in the ACC. To the extent that there are only small amounts of friction, mixing, and buoyancy-driven upwelling taking place in the real world, there should be only a small amount of deep diapcynal downwelling north of Drake Passage.